Effects of Mechanical and Thermal Forcing on the Enhancement and Ingredients of Orographic Rain Associated with the 2007-08 Madden-Julian Oscillation Passing the New Guinea Highlands

Justin G. Riley[1] & Yuh-Lang Lin[1]

[1] Department of Physics and Applied Science & Technology Ph.D. Program, North Carolina A&T State University, Greensboro, North Carolina, USA

Correspondence: Yuh-Lang Lin, 302H Gibbs Hall, AST Ph.D. Program, NCAT, Greensboro, NC, 27411, USA. E-mail: ylin@ncat.edu

Abstract

In this study, the Advanced Research Weather Research and Forecasting (WRF) model was adopted to investigate the mechanical and thermal forcing effects associated with the New Guinea Highland (NGH) on Madden-Julian Oscillation (MJO) propagation and rainfall formation and enhancement mechanisms over the island of New Guinea. Our results show that both forces affect the propagation of the MJO07-08, resulting in orographic rainfall production. Even though each forcing helps produce orographic rainfall, the mechanical forcing of the NGH plays a much larger role in the orographic blocking than the thermal forcing. We also found two flow regimes associated with the propagation of MJO07-08 over the NGH. First, in the flow-around regime, the MJO and its associated convective system split around the NGH due to the strong orographic blocking. We can observe this splitting when looking at the splitting stage. Second, the flow-over regime could occur when the mountain is lower than its original height or the flow has a smaller Froude number. A series of numerical experiments indicate that the maximum orographic rainfall increases with increased mountain height; however, the maximum orographic rain decreases when the flow transitions to the flow-around regime. Finally, some common ingredients for orographic rainfall associated with the MJO07-08 passing over the NGH are consistent with those found for tropical cyclones passing over mountains.

Keywords: orographic rain, Madden-Julian Oscillation (MJO), New Guinea Highlands (NGH), common ingredients

1. Introduction

Lin et al. (2020; denoted as L20 hereafter) studied the orographic effects on the propagation and rainfall modification associated with the Madden-Julian Oscillation 2007-08 (MJO07-08) passing over the New Guinea Highland (NGH). They found that the MJO07-08 went through three stages, i.e., blocking, splitting, and merging stages when it passed over the NGH. During the *blocking stage*, the propagation of the MJO was slowed, which led the flow and the MJO convection to the *splitting stage*, and then the *merging stage* when the MJO arrived at the southeastern corner of the NGH. However, the thermal forcing in the planetary boundary layer was not being investigated by L20; thus, it remains to be explored. In addition, L20 focused on the propagation and structure changes in the precipitating systems, but not the orographic rainfall mechanisms, such as the effects of diurnal thermal forcing associated with the orography on the MJO, the enhancement of orographic rain associated with MJO's passing over the NGH, and the common ingredients of orographic rainfall.

In past studies (e.g., Zhang and Ling 2017), the MJO over the Maritime Continent (MC) is separated into two distinct groups: (a) MJO-C: the MJO propagates over the MC continuously, and (b) MJO-B: which different from MJO-C, the MJO is blocked by the MC. Zhang and Ling (2017) found that MJO-B's rainfall is much higher over the sea than over the land. On the other hand, the MJO-C's rainfall over the ocean is never dominant. This suggests that the MC is inhibiting convective development over the sea could be a possible mechanism for the MC's barrier effect. Therefore, it was proposed that the rainfall over the ocean is caused by the land/sea breeze associated with the islands. Ling et al. (2019) investigated the effect of the diurnal cycle inland convection on the propagation of the MJO over the Maritime Continent Convective diurnal Cycle (MACCC) mechanism, i.e., the

diurnal cycle inland convection acts as an intrinsic barrier effect on MJO propagation over the MC. Precisely speaking, the barrier effects should include both mechanical blocking effect and diurnal thermal forcing effect. In the studies of Zhang and Ling (2017) and Ling et al. (2019), however, only focused on diurnal thermal forcing effects. Thus, there is a need to differentiate these two forcing mechanisms. In other words, the thermal effect of the NGH was not investigated, which deserves to be studied.

Based on the above discussion, in this study, we would like to address: (a) what is the relative importance between orographic blocking and diurnal thermal forcing? (b) What impacts of the diurnal thermal forcing on the orographic rainfall propagation and modification? In this study, we will be using mesoscale simulations with sensitivity tests to differentiate these two forces, such as removing the mountains and deactivating the diurnal heating and cooling. In addition, the modification of orographic rain associated with MJO will be investigated to understand how much the NGH enhances or weakens the orographic rain as an MJO passes over the island. Lin (2007) shows that the enhancement mechanisms of orographic precipitation are extremely complicated and are highly dependent on multiple factors. To study this, we will be looking at the no mountain (NoMT) results and sensitivity tests with varying mountain heights and comparing them to control case (CNTL) results.

Another scientific problem we would like to address is distinguishing between flow-over and flow-around precipitating systems (2D and 3D flow regimes) (Smolarkiewicz and Rotunno 1989). Chu and Lin (2000) found that there are three moist flow regimes for a conditionally unstable flow over an idealized 2D mountain; (1) An upstream-propagating convective precipitation system, (2) A quasi-stationary convective system over the mountain, (3) A quasi-stationary convective system in the vicinity of the mountain peak along with the downstream-propagating convective system. The first regime is explained by the convectively triggered cells upstream of the mountain due to an upstream-propagating density current formed by the evaporative cooling process. The second regime is a force balance between the orographic forcing and the cold-air outflow that plays a role in the quasi-steady precipitation concentrated over the mountain. In the third regime, the propagating rainfall is caused by the convection triggered ahead of the hydraulic jump over the lee slope, then advected by the basic flow. Chu and Lin found these three regimes are controlled by the basic-flow speed (U), the mountain height (h), and the upstream moist Brunt-Vaisala frequency (N_w) of the environmental flow parameters, which could be represented by one nondimensional, moist Froude number, $F_w = U/(N_w h)$. In extending Chu and 'Lin's study, Chen and Lin (2005b) adopted the upstream unsaturated moist Froude number (Emanuel 1994), $N_w^2 = (g/\theta)(\partial \theta_v/\partial z)$, where g is the gravitational acceleration, and θ_v is the virtual potential temperature to avoid negative values. Chen and Lin (2005b) included the convective available potential energy (CAPE) in addition to the moist Froude number (F_w). They identified four conditions unstable flow regimes over an idealized 2D mountain. The interplay explains the flow characteristics among the orographic blocking, the precipitation system's advection, and the density current forcing. Their results showed that large horizontal wind speeds could modulate the orographic precipitation under a low-CAPE flow. Their findings imply that the precipitating system does not require a high CAPE to produce heavy orographic rainfall (Huang and Lin, 2014). However, the flow responses and associated orographic rain behavior differ from a three-dimensional mountain (3D).

The study of Chen and Lin (2005b) was extended by Chen et al. (2008) to examine the flow regimes over a three-dimensional (3D) mountain. Their study included two flow control parameters, F_w and h/a (mountain aspect ratio of the mountain height and half-width). Miglietta and Rotunno (2009) performed a series of simulations of a conditionally unstable flow impinging on a mesoscale ridge on a 3D domain and a high resolution to resolve cellular-scale features properly. The overall flow characteristics in their results were consistent with those in Chu and Lin (2000). In addition, they also found that a functional dependence of the rainfall rate was caused by three parameters: the triggering and orographic forcing of the convection and the convective time scales' advection ratio. Thus, both studies helped the understanding of orographic rainfall dynamics. We try to address in this study whether the results found in those idealized numerical studies can be applied to those that happened in the real atmosphere.

Numerical studies have demonstrated that reducing the effective static stability of a moist flow may increase the release of latent heating, which, in turn, force the flow to transition from flow-around a higher mountain ridge to flow-over lower mountain ridge (Buzzi et al. 1998). Therefore, the study of L20 implied that an MJO might pass over the NGH, depending upon the Froude number. As discussed above, the thermal forcing plays a critical role in the barrier effect. In this study, we are interested in the thermal forcing associated with the diurnal variation associated with the sea surface temperature (SST) by updating the SST every 12 or 6 hours in the mesoscale model instead of no SST variation as assumed in L20. The sensitivity experiments on diurnal heating and cooling associated with orography may help differentiate the mechanical and thermal forcing on the orographic blocking

and then orographic enhancement of MJO precipitation.

Because MJO07-08 went through a blocking stage after interacting with the northwest (NW) corner of NGH, we would like to investigate the orographic impacts on the orographic rainfall, including orographic initiation and enhancement, the NW corner of the NGH. The orographic forcing on the incoming airstream is highly dependent on the detailed geometry of the mountain (Lin 2007). Lin (2007) also showed that the amount and distribution of the orographic tropical cyclone (TC) precipitation strongly depends on the TC's synoptic environment during its passage over a mountain range, but can we use this idea for MJO. To help us understand the orographic influence on rainfall on the NW corner of New Guinea, we will help us with the ingredient approach discussed in Lin et al. (2001). The following equation determines the orographic precipitation (P):

$$P = \varepsilon \left(\frac{\rho_a}{\rho_w}\right) (V_H \cdot \nabla h + w_{env}) \left(\frac{L_s}{c_s}\right) q_v, \tag{1}$$

Where ρ_a and ρ_w are the liquid water density and air density, respectively, ε is the precipitation efficiency, w_{oro} and w_{env} are the vertical velocities forced by orography and environment, respectively, q_v is the water vapor mixing ratio, L_s and c_s are the horizontal scale of the precipitating system and its moving speed, respectively. To examine the ingredients of orographic rainfall of the NW corner of the NGH, we will use a fine-resolution set, such as 1km, mesoscale model-simulated parameters.

In this study, we will use the Advanced Research Weather Research and Forecasting (WRF) model (Skamarock et al. 2019) to examine the orographic and thermal effects of the NGH on MJO propagation and rainfall over the island of New Guinea. First, we will discuss the model description and experimental design in section 2. This will also include the model verification of each of the sensitivity cases. Next, in section 3, we will analyze the numerically simulated results to study the mechanical and diurnal thermal forcing associated with the orography on MJO, the enhancement of orographic rain associated with MJO passing over the NGH, and the ingredients of orographic rainfall on the NW corner of the NGH. Finally, we will be presenting the concluding remarks of our study in section 4.

2. Model Description, Numerical Experiment Design, and Model Verification

2.1 Model Description

The WRF model version 3.9.1 (Skamarock et al. 2019) is adopted for the numerical simulations of MJO07-08 and its associated rainfall and propagation over the NGH, which possesses the following key characteristics:

- A numerical weather prediction system was developed to help with better mesoscale weather.
- It incorporates initial idealized data or better forecasting weather by incorporating initial real data into the model.
- It is a three-dimensional, non-hydrostatic, fully compressible model that uses terrain-following vertical coordinates with stretched grid resolution, one or two-way multiple-nesting capability, options for upper and lateral boundary conditions, etc.
- The model equations are written in flux-form with conserved mass and dry entropy.

Thus, the WRF model provides a flexible and robust platform for operational forecasting while offering more options in the advanced scheme in physics parameterizations and numerical methods, including data assimilation techniques.
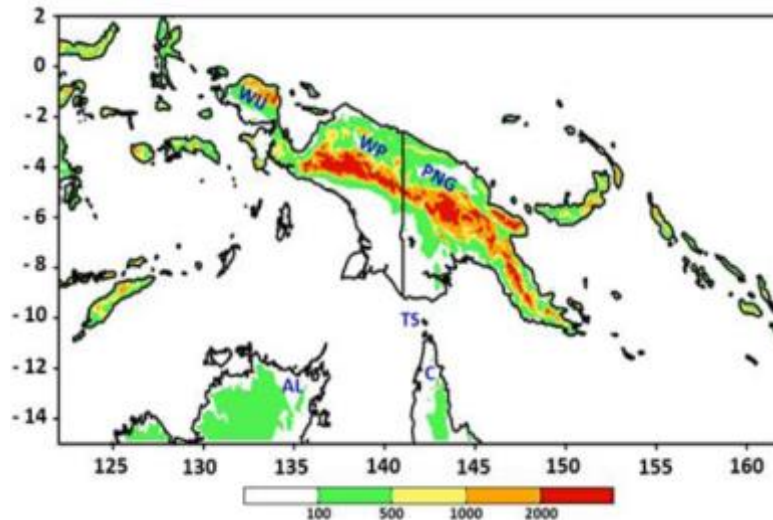
Figure 1. The model domain and topography of New Guinea Highland (NGH) extend from northwest of New Guinea to the southeast with the highest peak of 4884 m. The terrain height is in m. The topography of regions denoted in this domain is WP: West Papua; WIJ: West Irian 679 Jaya (northwest peninsula of the West Papua); PNG: Papua New Guinea; PNG: Papua New Guinea; AL: The Arnhem Land of Australia; C: Cape York Peninsula of Australia and TS: Torres Strait

2.2 Numerical Experiment Design

For the first mesoscale simulation performed in this study, the domain is the same as L20. The focus area is the NGH, the largest island of the MC, and its surrounding areas. Only one domain is designed for our mesoscale simulations, which is from the southwest corner (122ºE, -15ºS) to northeast corner (162ºE, 2ºN) consisting of 887 x 376 horizontal grid points with 5km horizontal grid resolution, 32 vertically stretched grid levels, and 30 s time interval. The domain and NGH terrain are shown in Fig. 1. The domain was designed to resolve the MJO event of 2007-08 (MJO07-08), described in L20; the NGH and orographic impacts of MJO can be simulated in more detail the event propagates eastward across the mountains. The physics parameterization schemes used for the simulation are the same as those in L20: (a) cumulus: Grell 3D, (b) microphysics: WSM6, (c) planetary boundary layer: YSU, (d) surface layer: Monin-Obukov, (e) longwave radiation: RRTM, and (f) shortwave radiation: RRTMG. Details of the selected schemes can be found in the WRF user's manual (Skamarock et al., 2019). Unlike the global model simulations used in previous studies, the combination of the domain, grid resolution, and physics parameterization schemes allow us to study mesoscale dynamics associated with the passage of the MJO07-08 over the NGH. The mesoscale model was initiated with ECMWF interim data, and the boundary conditions were updated for six days (12/29/00Z/07-1/4/00Z/08). This period was described in L20 as when the MJO passed over the NGH. Several sensitivity cases were run and will be discussed in the following sections to answer the proposed questions in this study.

2.3 Model Verification

The experimental design of the CNTL case is identical to that of the L20 except that the SST data is updated every 6 hrs after the model initiation since we found that updating the SST at a finer time interval has improved numerical simulation results in other similar studies. In addition, the WRF model does not predict the SST during the simulation, meaning updating the SST during the simulation run will give us a more accurate look that the environment as the MJO propagates over the NGH. If the SST updating case results prove to improve the results found in L20, then this case will serve as the control case (CNTL) for the remainder of the study. SST updating will also be used in other sensitivity tests discussed later.
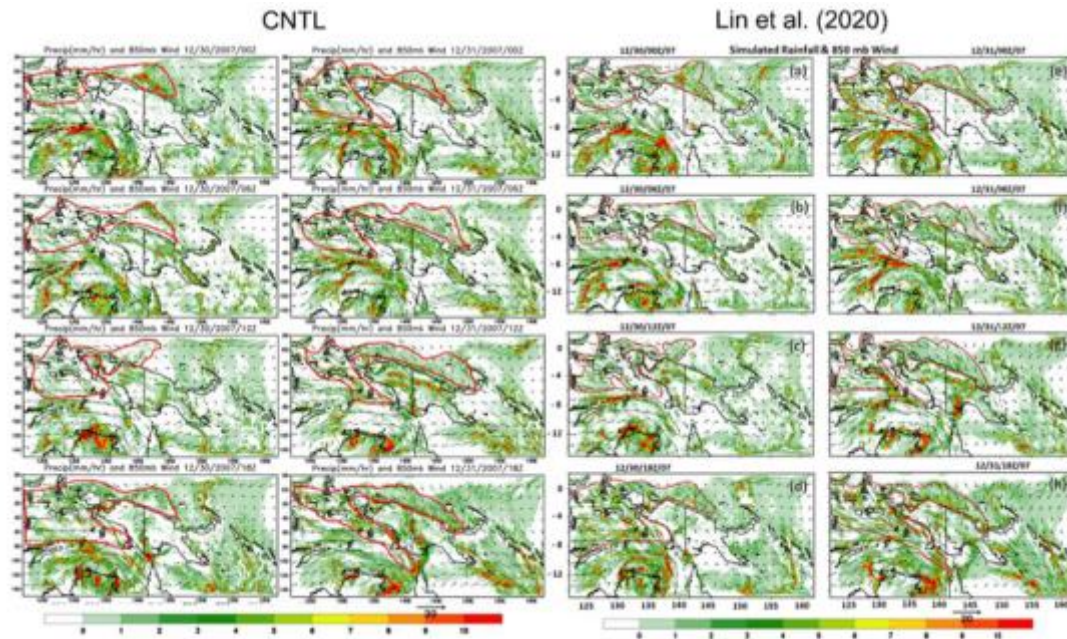
Figure 2. Simulated rainfall fields (12/30/00Z – 12/31/18Z 2007) in CNTL (left) and L20 (right)

The WRF-simulated CNTL results are verified by the Tropical Rainfall Measuring Mission (TRMM) 3B42 v7 data, the NOAA-Interpolated OLR data, and the wind vectors data. For the TRMM data, the temporal resolution used is three-hourly data from 12/30/07 to 1/4/08. Its spatial resolution is a 0.25 latitude-longitude grid. For the NOAA-Interpolated OLR, the temporal resolution used is daily data from 12/30/07 to 1/4/08. Its spatial resolution is a 2.5 ° latitude-longitude grid. We will also compare the WRF-simulated results of the control case to the results found in the L20 paper.

Verification of the simulated MJO passing over the NGH includes precipitation, total water content, and outgoing longwave radiation (OLR). When comparing the CNTL simulated rainfall fields to those of L20 (Fig. 2), the CNTL results show slightly more rainfall along the NGH and the coast during the blocking stage MJO07-08. When comparing the results to TRMM, their rainfall patterns are similar in the same period. When comparing the rainfall from the CNTL case to L20 and the TRMM data, the CNTL case, which updated SST data, improves the MJO event's model simulation. There is only a slight increase in rainfall in the simulation. However, the rainfall pattern seen in the TRRM observational data results is also present in the CNTL case. This indicates that updating the SST data has improved the simulation of the rainfall structure.

The OLR (Fig. 3) results also show a slight increase in the number of deep clouds along the NGH compared to L20 OLR results. When looking at L20 during the blocking stage, we can see that during the day of 12/31/08 at 12Z, a large deep convection cloud forms on the southwest side of the island of New Guinea. However, during the simulation run of the CNTL case, that large deep cloud does not form in that island area. The OLR pattern is like the pattern seen in the OLR observational data (Fig. 3). These are present when looking at all three stages that MJO07-08 goes through during its eastward propagation. Updating the SST data also helps simulate the deep convective clouds associated with MJO07-08 and produce results like the OLR observational data. The verification of the CNTL case shows that updating the SST data during the simulation every 6 hours improved the results seen in L20. Thus, the simulation can be used to research this study.
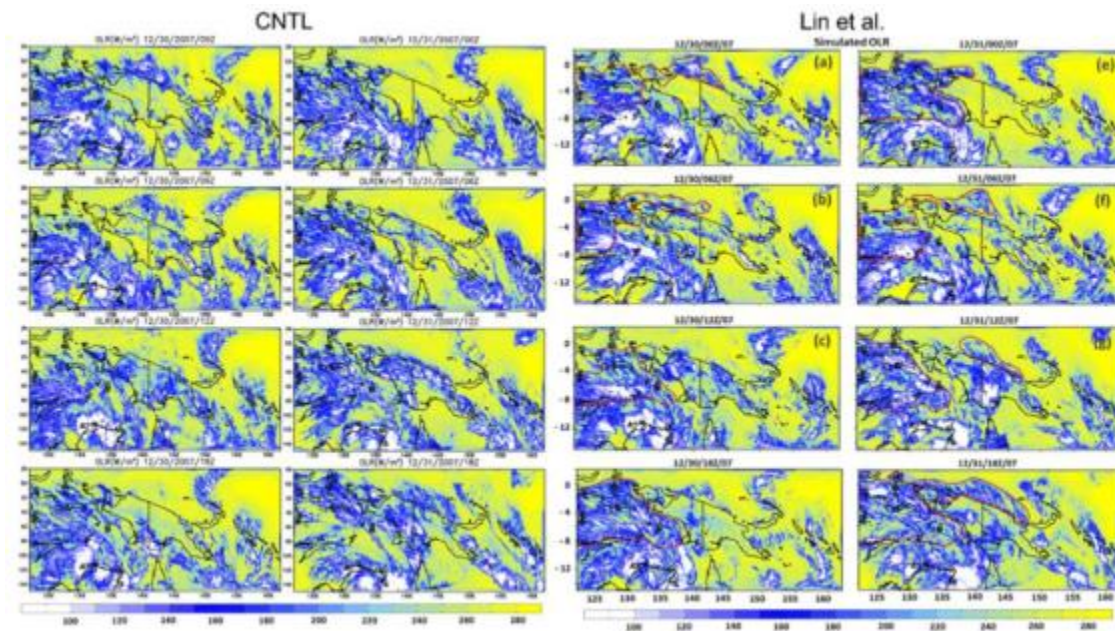
Figure 3. OLR fields (12/30/00Z – 12/31/18Z 2007) simulated in CNTL (left) and L20 (right)

3. Results

3.1 Mechanical and Diurnal Thermal Forcing Associated with the Orography on MJO07-08

Jiang (2012) showed that while passing over the island of New Guinea, MJO07-08 is split into two systems and passed over the island along the northeast and southwest coasts. Once MJO07-08 passed over the island, these two split convective systems of the MJO merged to the southeast of New Guinea. Thus, the MJO passed over New Guinea occurred approximately 12/31/07 – 1/5/08.

From 12/21/07 – 1/10/08, the MJO appeared to jump over the MC instead of moving smoothly over it. As MJO07-08 propagates over the island of New Guinea, we can see it being blocked by the NGH before proceeding through the three stages described by L20 and then continuing its eastward propagation. This can be seen in Jiang's (2012) research, where they showed the propagation of the MJO using a Hovmöller diagram (Fig 4.). From the diagram, we can see that the MJO propagation takes over a month (12/01/07 - 01/10/08) to propagate over the MC completely, and we see the MJO event go through the blocking, splitting, and merging stages as it interacts with the island and NGH. For this research, we will be looking at the blocking and splitting stages described in L20 when looking at the mechanical and thermal forcing that affects the eastward propagations.

The blocking of the MJO is caused by the mechanical and thermal forcing of the NGH. Because of these two forces acting upon the propagation of MJO07-08, we must differentiate the difference between the mechanical and thermal forces. The mechanical forcing is caused by the interaction of the MJO and the orographic terrain of the NGH. The thermal forcing is caused by the diurnal heating/cooling of the island. This is mostly seen through the sea and land breeze interaction. To differentiate the mechanical and thermal forcing of the NGH on the MJO, we will perform three sensitivity tests using the same WRF model and domain defined for this study. Each test will investigate the impact of each force and how it impacts the MJO system during its eastward propagation.

The first sensitivity test performed is the no mountain case (NoMT). As discussed in L20 and summarized in the Introduction, the MJO went through three stages propagating over the NGH. The NoMT case will show if the MJO still goes through those stages and how to impact the orographic terrain of the NGH has on the MJO.

The second sensitivity test that will be performed is the no diurnal heating case (NoHT). The NoHT case will study the impacts of diurnal heating on the MJO as it propagates over the NGH. This test will investigate the MC's barrier effects on the MJO propagation, which is sometimes seen when the MJO propagates through the MC. We will also look at the sea and land breeze interaction with the MJO and its effects on the rainfall associated with the MJO system. A sea breeze is when the wind blows from the ocean and toward the landmass of the island of New Guinea, and the land breeze is the reverse effect of the sea breeze, where we see the wind

blowing from the island and toward the ocean. The second test will also help us see which of the two forcing is the most dominant impact on the MJO system propagating over the island. The theory is that forcing plays a part in blocking MJO07-08, but mechanical forcing plays a bigger part than thermal forcing.

The final sensitivity test case is to deactivate the diurnal heating and remove the mountain (NHNM). This sensitivity test will explore the flow behavior under no mechanical and thermal forcing during the propagation of the MJO over the NGH. We anticipate seeing that the MJO is freely passing over the island of New Guinea with no blocking and slow-down of its propagation speed and no impacts on the rainfall associated with the MJO. These sensitivity experiments and their key characteristics are summarized in Table 1.

Table 1. The control and all the sensitivity cases performed in this study

Case	Key Properties
CNTL	This serves as the control case, which is initialized by the ECMWF-interim data with SST updated every 6 hrs.
NoMT	Same as the CNTL case, except the mountains are removed.
NoHT	Same as the control case, but there is no diurnal heating and cooling in the WRF simulation.
NHNM	No mountains and No diurnal heating and cooling
87.5MT*	Same as the CNTL case, except the mountains are reduced to 87.5% of their original heights.
75MT	Same as the 87.5MT* case except for 75% reduction.
62.5MT*	Same as the 87.5MT* case except for 62.5% reduction.
50MT	Same as the 87.5MT* case except for 50% reduction.
37.5MT*	Same as the 87.5MT* case except for 37.5% reduction.
25MT	Same as the 87.5MT* case except for 25% reduction.
12.5MT*	Same as the 87.5MT* case except for 12.5% reduction.

* The sensitivity tests used for the Froude number discussions.

3.1.1 The Impact of Mechanical Forcing on MJO07-08

The NoMT case was performed to see how much of an impact the mechanical forcing of the NGH has on MJO07-08. At first glance, when comparing the CNTL case to the NoMT case (Fig. 4), we can see a clear difference in how the MJO interacts with the island when there is no mountain compared to when the NGH is in the domain. When comparing the two cases, the first thing that we observed is the wind flow direction during its propagation. When looking at the NoMT case, the wind flow is across the island compared to the CNTL case, where we see the wind flow around the NGH. Without obstructing the mountains in the NoMT case, the flow can easily move across the island without being blocked by the orographic terrain. This allows the MJO to propagate easily across the island and allows the MJO to move along the flow direction. We can see this during the blocking stage of MJO07-08, wherein the NoMT case the deeper clouds and rainfall associated with the MJO can be located on the southeast (SE) portion of the New Guinea island. Unlike the CNTL case, where the deep clouds and rainfall can be seen on the island, the orographic rain produced as MJO07-08 interacts with the NGH. The propagation speed of MJO07-08 has also increased with the removal of the NGH. In the CNTL, the propagation of MJO07-08 is ~5 m/s, which the average propagation speed of the MJO propagates through the MC. With the terrain removed, the propagation speed of MJO07-08 is ~9 m/s.
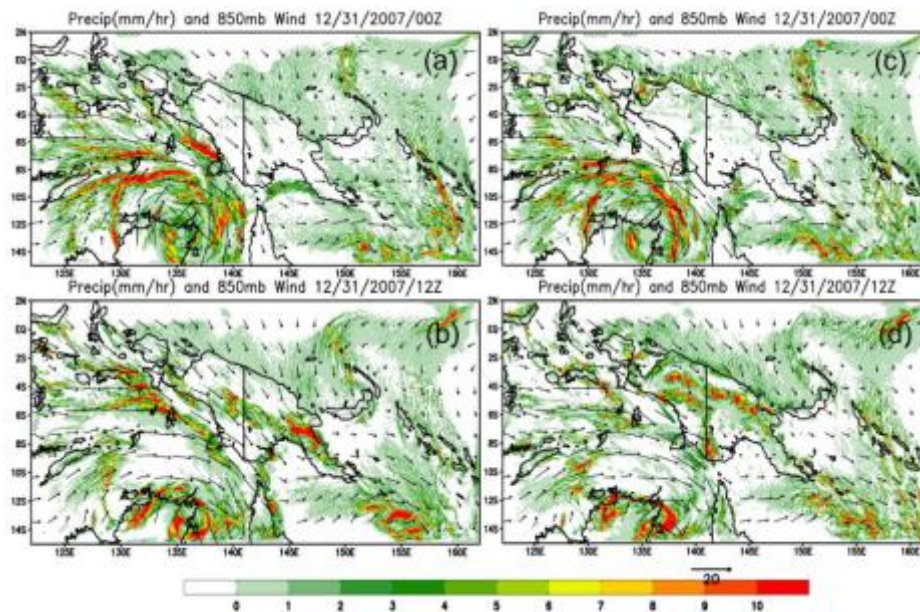
Figure 4. The 3-hour rainfall and 850mb wind fields during the blocking stage of MJO07-08. Panels (a) and (b) are the NoMT case for 12/31/00Z and 12Z 2007, respectively, and (c) and (d) is the same as (a) and (b) except for the CNTL case

In discussing the rain associated with MJO07-08, we must identify the three types of rain associated with this case. The types of rain associated with this case are (1) MJO-R, the rain associated with the MJO. (2) Oro-Rain, which is the rain caused by the diurnal heating of the mountain. (3) TC-Rain is the rain associated with the TC-Elizabeth located south of the island of Papua New Guinea. We are not worried about the TC-Rain during the MJO07-08 case for this study. However, we need to point the TC-Rain out because TC Elizabeth occurred simultaneously when the MJO propagated over the island. Therefore, our research is only focused on the first two types of rain.

The NoMT case also shows how much the mechanical forcing of the NGH impacts the rainfall associated with MJO07-08. In the NoMT case, there is no production of orographic rainfall in the simulation results. This is due in part to the removal of the NGH. This does reduce the amount of rainfall in the simulation. However, when looking at the rainfall in the NoMT case, we can see an increase in rainfall of the island's southwest (SW) coast compared to the CNTL case. This can be attributed to the weakened blocking effect of the island, allowing the rainfall associated with MJO07-08 to be more clustered together in a massive convective system. This is compared to the CNTL case, where the rainfall is scattered along the mountain chain because we still have the NGH in the simulation. The NoMT case only has the MJO-R type of rain observed in the simulation, unlike the CNTL case, where we have both the MJO-R and the Oro-Rain. The only force affecting MJO07-08 is the thermal forcing caused by diurnal heating and cooling. However, the thermal forcing is not strong enough to block MJO07-08. The blocking stage and the massive convective system (MCS) can easily propagate over the island. Therefore, the rainfall seen in the rainfall plots for the NoMT case is not orographic rain like what can be observed in the CNTL case along the NGH. The rainfall on the SE portion of the island is the MJO-Rain as the MCS propagates across the island. The rainfall on the island's SE seems to be more compacted in the SE due to convergence produced by the current cyclonic flow in the area. This cyclonic flow is due to the weakened sea breeze interaction with the east's incoming flow. This newly developed cyclonic flow also increases rainfall as MJO07-08 propagates through that area.

However, the increased rainfall off the coast and on the island's SW does not mean that the blocking effect is no longer present. There is still thermal forcing present, affecting the propagation of MJO07-08. However, due to the removal of the terrain in the NoMT case, the thermal forcing from the land/sea breeze has been weakened. This allows MJO07-08 to propagate rather smoothly over the island with an increased propagation speed. When studying the OLR results (Fig. 5), the deep clouds associated with the MJO07-08 are closer to the island's SW coast than the CNTL case, where the deep cloud of the MJO is farther from the coast. The Hovmöller diagram shows how the propagation of the deep clouds associated with MJO07-08 is uninterrupted as it begins to interact

with the island of New Guinea. Once again, this is caused by the weakened thermal forcing present in the NoMT case.
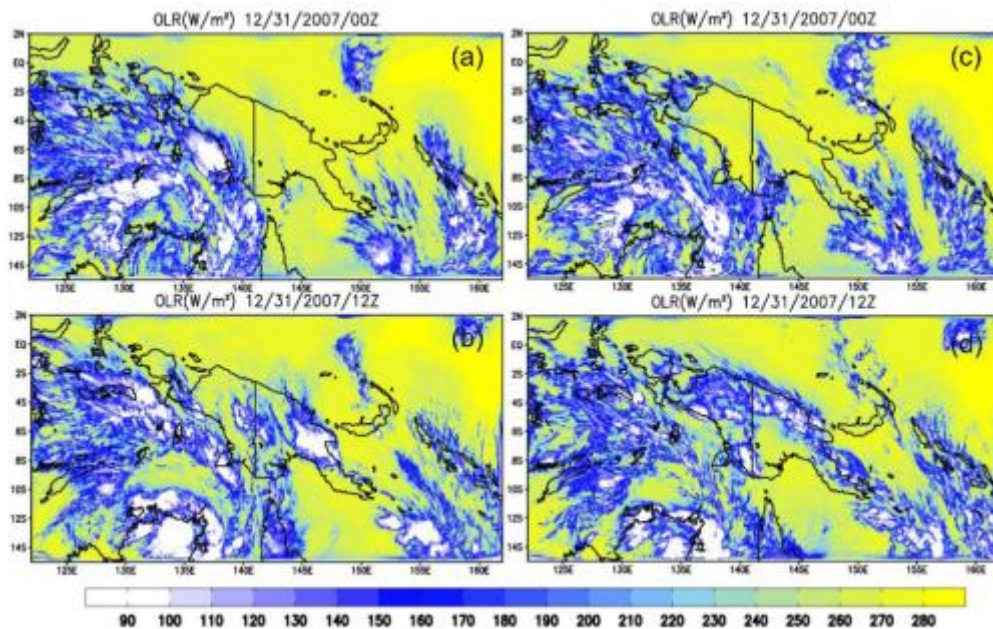

Figure 5. Outgoing Longwave Radiation during the blocking stage of MJO07-08. (a) and (b) are the NoMT case for 01/02/00Z and 12Z 2008, respectively, and (c) and (d) is the same as (a) and (b) except for the CNTL case
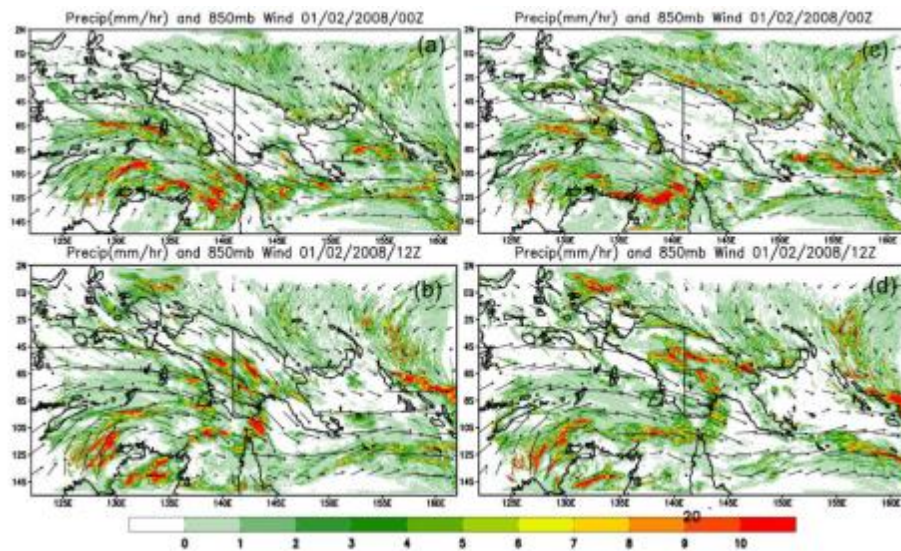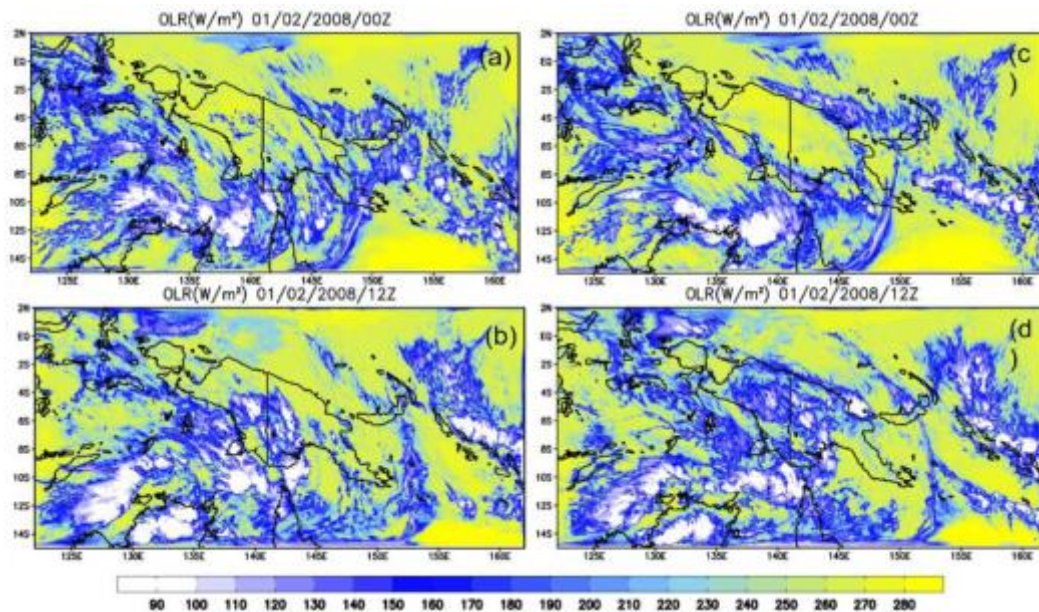

Figure 6. The 3-hour Rainfall and 850mb wind during the splitting stage of MJO07-08. (a) and (b) are the NoMT case for 01/02/2008 00Z and 12Z, respectively, and (c) and (d) is the same as (a) and (b) except for the CNTL case

Figure 7 shows the 3-hour rainfall and 850 mb wind fields during the splitting stage of the MJO07-08, as simulated by the WRF model when comparing the splitting stage of the NoMT case to the splitting stage of the CNTL case, we can first look at the rainfall for both cases (Fig. 6). During the splitting stage, the MJO07-08 continuously propagates over the island on its eastward propagation. Due to the weakened thermal forcing present, the NoMT case's rainfall is more centralized at the island's southeast (SE) portion. Therefore, there is no splitting of the MCS into two separate convective systems present in the NoMT case. Because of this, the flow propagation is over the island, and MJO07-08 can easily move over the island of New Guinea. During the

splitting stage, the MJO07-08 continuously propagates over the island on its eastward propagation. Due to the weakened thermal forcing present, the NoMT case's rainfall is more centralized at the island's southeast (SE) portion. Therefore, there is no splitting of the MCS into two separate convective systems present in the NoMT case. The 850mb winds also show that the northwest (NW) easily flows over the island since it is no longer blocked by the orographic of the island of New Guinea. Compared to the winds observed in the CNTL, where the NW flow is forced around the NGH, and there is little to no wind located on the island in the CNTL, which is due to the high and complex terrain the NGH.

Figure 7. Outgoing Longwave Radiation during the splitting stage of MJO07-08. (a) and (b) are the NoMT case for 01/02/00Z and 12Z 2008, respectively, and (c) and (d) are the same as (a) and (b) except for the CNTL case

When comparing the OLR during the splitting stage for both the CNTL and NoMT (Fig. 7), the deep convective clouds associated with MJO07-08 are more collected into a larger MCS located in the southern part island (Fig. 7d). However, unlike the CNTL case, we can see the separation of the MCS into two separate convective systems. This is because the flow can propagate over the island without being blocked by any complex terrains. Also, because of the weakened thermal forcing of the island, the MCS of MJO07-08 can move as one entity during its eastward propagation. Compared to the CNTL case, where because of the mechanical and thermal forcing of the NGH and island, respectively, MJO07-08 is forced to split around the island after it becomes blocked and stalled by the orographic effects of the NGH. The NoMT case has shown that there is blocking from the thermal forcing of the island of New Guinea, but the thermal forcing itself is not enough to cause the MJO event to go through the three stages seen in the L20 paper.

3.1.2 The Impact of Thermal Forcing on MJO07-08

In past studies, such as Zhang and Ling (2017), the heavy rainfall produced by blocking could be caused by the island's land/sea breeze interaction (Fig. 11 of Zhang and Ling). However, many studies only look at the thermal forcing impacting the MJO. With the NoHT case, we want to know how significant the impact of the thermal forcing is compared to the mechanical forcing of the NGH. If the thermal forcing is shown to play a large impact in the blocking of MJO07-08, this would mean that there would be the presence of a barrier effect around the island. If not, then that would suggest that either the mechanical forcing plays a larger part or a combination of the two forces.

When compared with the CNTL case, the blocking effect in the NoHT was still present when the MJO07-08 approached and interacted with the NGH. However, there is only a little orographic rainfall on the island and the mountain range. This indicates that no sea or land breeze was generated in the simulation. Lin (2007) reviews how the complicated interactions between orographic and thermal forcing influence the dynamics of the mountain-plains solenoidal (MPS) circulations. In addition, Lin (2007) indicates that sea and Land breezes may combine the orographically and thermally forced winds near the coasts of a mountainous island, including the slope and mountain valley winds. During the day, the mountain serves as an elevated heat source due to the

sensible heat released by the mountain surface. "In a quiescent atmosphere, this can induce mountain upslope flow or upslope wind, which in turn may initiate cumuli or thunderstorms over the mountain peak and produce orographic precipitation" (Lin 2007). In the CNTL case, the surface temperature and 900 mb winds (Fig. 8) show that a sea breeze occurred from 00Z to 12Z (10L to 22L, where L stands for the local time of Papua New Guinea), and there was a land breeze that occurred between from 15Z to 00Z the next day (01L to 10L).
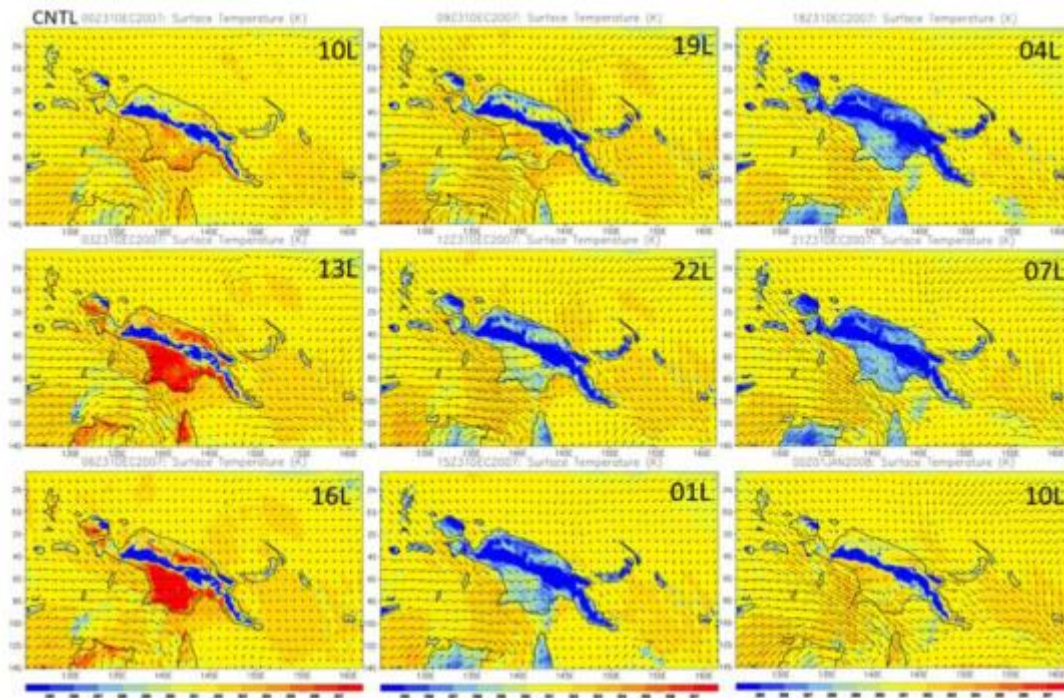
Figure 8. The 3-hour surface temperature and 900 mb winds for the CNTL case. (L denotes the local time on the island)
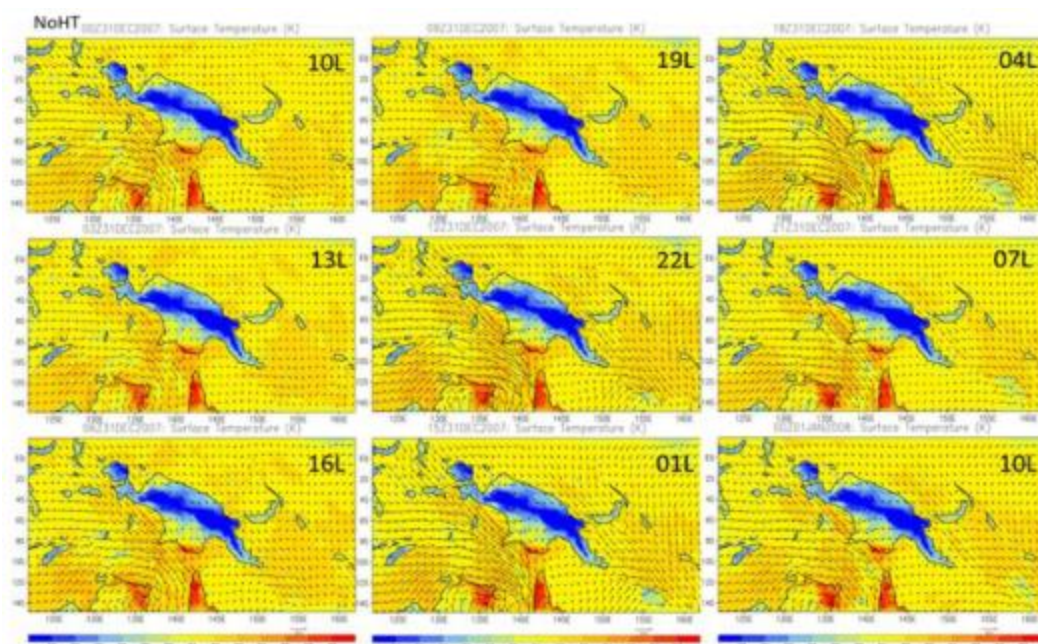
Figure 9. The 3-hour surface temperature and 900 mb winds for the NoHT case. (L represents the local time on the island)

When comparing the times where we observe the sea breeze interaction with the NGH to the 3hr precipitation plots (Fig. 4) during the blocking stage, we can see that a large amount of rainfall along the NGH corresponds to the strong sea breeze interaction with the NGH. On the other hand, during the land breeze interaction, we can see rainfall along the island's coast instead of along the NGH. This is like the results observed by Zhang and Ling when discussing the barrier effect for the MJO-B group. Thus, these results in the CNTL show that the thermal forcing from the NGH does play a part in the blocking of MJO07-08.

In the NoHT case, with the removal of the diurnal heating from the land, we observe no longer the sea and land breeze interaction like what was seen in the CNTL case. Because of this, the land remains much cooler than the surrounding ocean water, which can be seen in the surface temperature plots for the NoHT case (Fig 9). Because the land is much cooler than the surrounding ocean surface temperature, the thermal forcing associated with the blocking of the MJO is no longer affecting the MJO. Meaning that the only force affecting the MJO is the mechanical forcing.
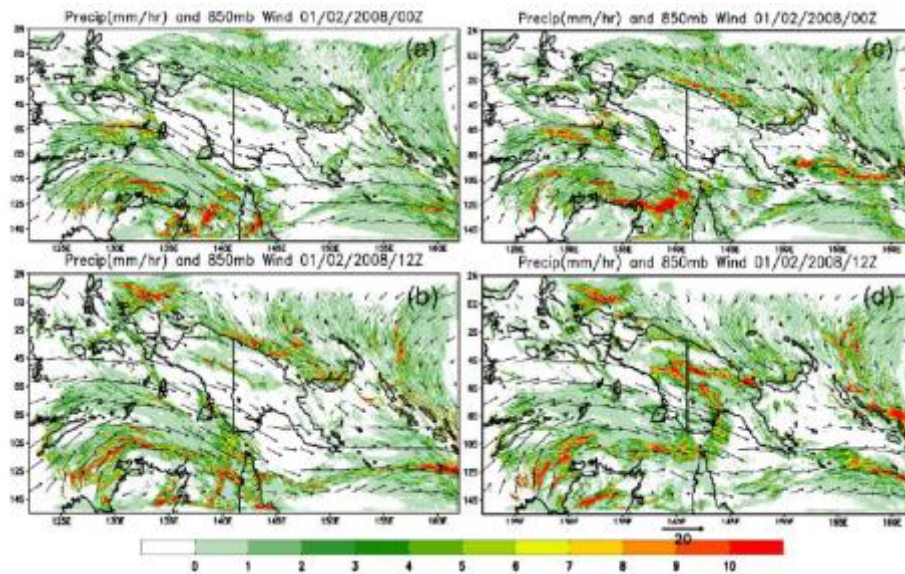

Figure 10. The 3-hour rainfall and 850mb wind fields during the blocking stage of MJO07-08. Panels (a) and (b) are the NoHT case for 01/02/00Z and 12Z 2008, respectively, and (c) and (d) is the same as (a) and (b) except for the CNTL case
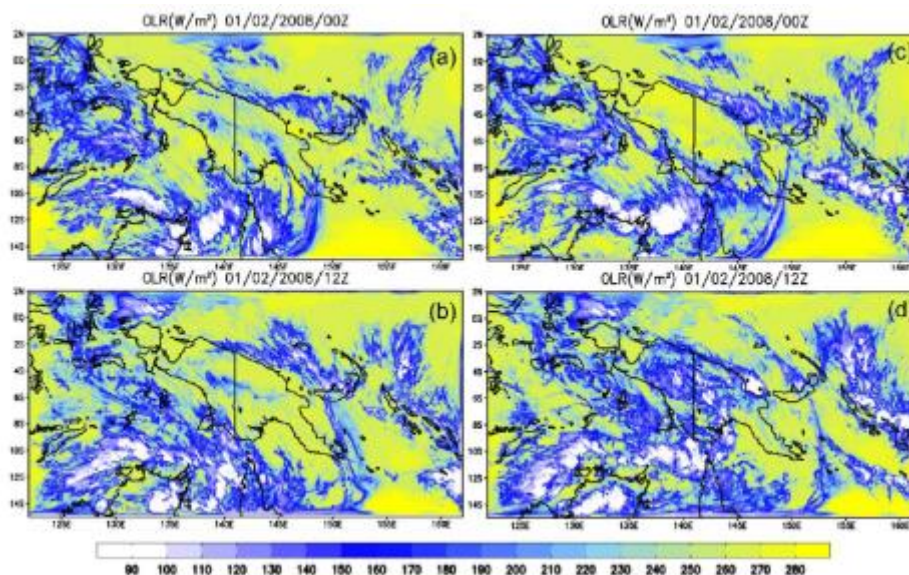

Figure 11. Outgoing Longwave Radiation during the blocking stage of MJO07-08. (a) and (b) are the NoHT case, and (c) and (d) are the CNTL case

With no sea breeze interaction with the NGH, orographic rainfall has been reduced drastically, but it is still orographic along the NGH. This shows that even though there is no longer a sea breeze to help with the production of orographic rainfall, the terrain and height of the NGH are complex and high enough to produce orographic rainfall. Also, when looking at the rainfall off of the island's coast, where we saw the land breeze interaction, the rainfall has been drastically reduced. This shows that the barrier effect has strengthened with removing the diurnal heating of the land. This also can be explained when looking at the 850 mb winds (Fig. 10) and the OLR plots (Fig. 11). There we can see that flow of the winds caused the deep convection of MJO07-08 to stay farther from the coast compared

To the CNTL and NoMT cases, respectively. This shows that, once again, the thermal forcing of the NGH does play a part in the blocking and splitting of MJO07-08. Unlike the results found in Zhang and Ling's (2017) research, the barrier effect seen with other islands does not seem to be present when looking at the orographic blocking of the MJO. However, this does not mean that the thermal forcing is the most important factor in orographic rainfall's blocking and splitting stages. When the diurnal heating is removed from the simulation, we can still observe orographic rainfall produced along the NGH. This hints that the mechanical and thermal forcing help each in the blocking and splitting of MJO07-08, with the mechanical forcing playing a large role than the thermal forcing.

3.1.3 The Impact of Mechanical and Thermal Forcing of MJO07-08

The NHNM case shows what happens to MJO07-08 when it is not impacted by the thermal or mechanical forcing of the island. As expected, MJO07-08 propagates along the SW flow and does not interact with the island. There is no orographic rainfall on the island when we see the sea breeze interaction. There is also no rainfall along the coast when we see the land breeze interaction. MJO07-08 also does not go to any of the stages described in L20. The MJO event can easily propagate across the domain, similar to the NoMT case. The NHNM case shows the importance of the thermal and mechanical forcing when blocking and splitting MJO07-08. The propagation of the MJO stays to the south of the island does not go through any of the stages described in L20. This also means that the MJO07-08 does not split around the island and is continuous as it propagates. Also, there is no orographic rainfall or any rainfall over the island's land. This lack of rainfall over the land is the cause of no sea breeze during the simulation (Fig. 12). Meaning the absence of diurnal heating and orographic blocking causes the MJO normally as if there is no landmass interacting with the convective system. Some convergence can be seen on the SW corner of the island. This is due to the weakened sea breeze interacting with the incoming flow from the east. Because the incoming flow is much strong than the sea breeze, convergence is formed on the SW corner.
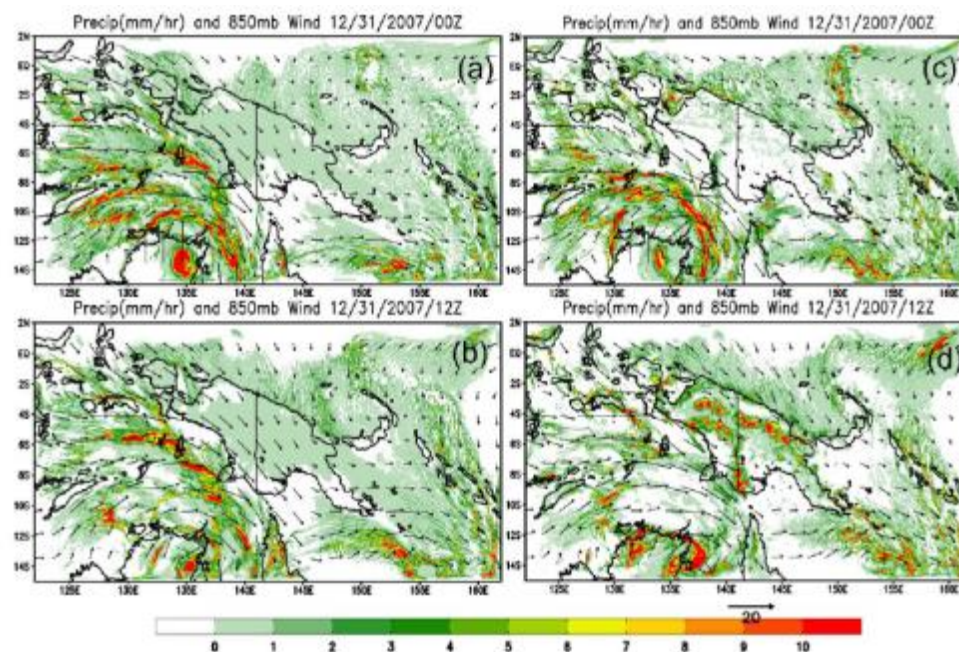

Figure 12. The 3-hour rainfall and 850mb wind during the blocking stage of MJO07-08. (a) and (b) are the NHNM case for 12/31/00Z and 12Z 2007, respectively, and (c) and (d) are the same as (a) and (b) except for the CNTL case

Comparing all the sensitivity tests to the CNTL case, there are some key facts that we can see when it comes to the impact of mechanical and thermal forcing of the island and the NGH. The first key fact is that the thermal forcing itself is not strong enough to block the eastward propagation of MJO07-08 completely. This would suggest a very weak barrier effect around the island of New Guinea, which would mean that the thermal forcing does not play a significant part in the production of heavy orographic rainfall. However, this does not mean that the thermal forcing does not contribute to heavy rainfall. When looking at the NoHT case, we can see that the mechanical forcing of the NGH by itself is strong enough to block the propagation of MJO07-08 completely. Looking at the OLR Hovm öller (Fig. 13), we can see that even when the thermal forcing is removed from the simulation, there is still strong blocking in the environment. This would mean that the mechanical forcing of NGH has a significant impact on the production of orographic rainfall. However, when looking at the three hourly rainfall plots (Fig 10. (c) and (d)), we can see that the amount of orographic rainfall has been reduced when the thermal forcing has been removed. This suggests that a combination of mechanical and thermal forcing is needed to produce orographic rainfall in the case of MJO07-08, with the mechanical forcing of the NGH playing a larger role in the orographic rainfall production than the thermal forcing.
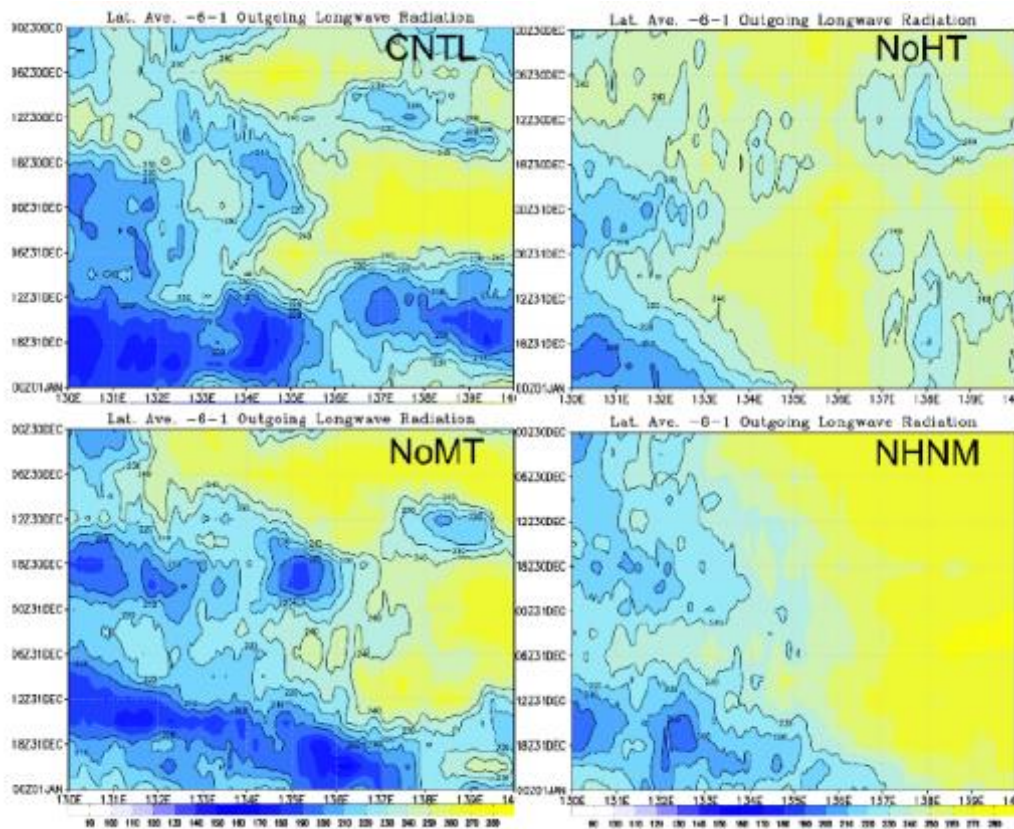

Figure 13. OLR Hovm öller diagram for each of the sensitivity cases

3.2 Modification of Orographic Rain Associated with MJO07-08 Passing Over the NGH

When looking at the enhancement of the orographic rain associated with MJO07-08 passing over the NGH, we can look at the flow regimes and orographic ingredients associated with the blocking stage. The CNTL and NoMT result from the previous section so that there is orographic blocking in the NW corner of the NGH during the blocking and splitting stages. To investigate how the orographic rainfall is modified, we will look at the flow regimes of the precipitating system and the orographic ingredients associated with the MJO07-08.

To differentiate the flow-around and flow-over precipitating systems, a slope analysis of the NGH was performed to show when the orographic rain is associated with the MJO07-08 transition between three-dimensional flow and two-dimensional flow. To perform the slope analysis, three simulations were done with varying heights. The cases and how much the heights vary per case can be seen in Table 1. With these varying heights, we calculated the Froude number, which was defined earlier, for each of the cases represented in

Table 2. We also used the NoMT case for comparison, even though the Froude number of the NoMT case would be infinite. Finally, calculated the mountain height-length aspect ratio ($S = h/L$) for each case to compare to determine the flow regimes for each case.

This process is like what Chen and Lin (2008) performed for their study. However, there are some key differences when comparing their study to ours. The first difference is that we are only looking at two flow regimes instead of the four flow regimes Chen and Lin (2008) found. Second, how the aspect ratios were found differs from those for their cases. Third, Chen and Lin (2008) used varying half-widths in their study to use varying mountain heights instead. Finally, Chen and Lin (2008) used an idealized mountain to conduct their study. However, this study's mountain is a real mountain using real data to imitative the WRF model. This means that our study only looks at two flow regimes for the MJO07-08 case. We deal with 3D flow regimes, not the 2D flow regimes shown in Chen and Lin's (2008) paper.

The 3D flow regimes that we are studying are the flow-around and flow-over regimes. Also, because our mountain is real, our aspect ratio is represented by equation (3). The flow-around regime can be described as when the MJO becomes blocked during the blocking stage. As a result, the convective flow splits around the mountain to continue its eastward propagation. This splitting is the same as described during the splitting stage described in L20. The flow-over regime is described as when the orographic terrain blocks the MJO. The blocking effect is weak enough that the convective flow continues over the mountain instead of splitting around the mountain.

During the study, we calculated the Froude number for each case with varying mountain heights, represented in Table 2 using the unsaturated Froude number, as defined earlier. We also used the NMNT case for comparison, even though the Froude number of the NMNT case would be infinite. We calculated the mountain height-length aspect ratio (h/L) for each case to compare to determine the flow regimes for each case. Flow flow-over (I) is seen when the mountain height is below 50% of the original mountain height. Flow regime flow-around (II) is seen when the mountain height is above 50% of the original mountain height. When the mountain is at 50% of the original height, the flow regime is in both I and II. This means that we can observe the MJO07-08 split around the NGH and flow over the NGH as well. This shows that the splitting occurs as the orographic terrain blocks the MJO07-08, mostly caused by the terrain itself and not by its diurnal thermal forcing. This is the opposite of what is discovered by Zhang and Ling (2017), which discusses the barrier effect to the island's thermal forcing. This does not mean their finds are wrong, but this barrier is not the main reason for the flow splitting regarding the NGH and the MJO07-08. In the case of the MJO07-08, the splitting of the convective flow is mainly caused by the mechanical forcing of the orographic terrain.

Table 2. The upstream Froude number of each sensitivity performed during the study and their aspect ratio and flow regime

Case	Froude Number (F_w)	Mountain Aspect Ratio (h/L)	Flow Regime
CNTL	0.244	0.060	Flow-around
87.5MT	0.279	0.052	Flow-around
75MT	0.325	0.045	Flow-around
62.5MT	0.390	0.038	Flow-around
50MT	0.488	0.030	Flow around/over
37.5MT	0.651	0.023	Flow-over
25MT	0.976	0.015	Flow-over
12.5MT	1.950	0.008	Flow-over
NoMT	∞	0	Flow-over

The orographic ingredients are also important in understanding the modification of orographic rainfall associated with the MJO07-08 propagating over the NGH. As discussed in the Introduction of this paper, Lin et al. (2001) formulated an equation that applied Doswell et al.'s (1996) ingredients approach to the upslope of orographic precipitation (equation 1), using common synoptic and mesoscale environment features favorable to heavy orographic rainfall in the United States. In Lin (2007), the study identifies that the occurrence of heavy orographic precipitation needs a combination of any of the following ingredients: (1) High precipitation efficiency (ε), (2) Strong orographic lifting (w_{oro}) or LLJ (U) and steep mountain ($\partial h/\partial x$) since $w_{oro} = \partial h/\partial x$, (3) Strong environmental lifting (w_{env}) (the release of conditional instability – large CAPE, potential instability, low-level convergence, and upper-level divergence), (4) Large moist airflow upstream (qv), (5) Large preexisting convective system (Ls), and (6) Slow translational motion of the storm (c_s). With the MJO07-08 being an MCS

that slowly propagates over the NGH, we can confirm that the last two ingredients, the large preexisting convective system and the slow translational motion of the storm, are important ingredients to the production of orographic rainfall.
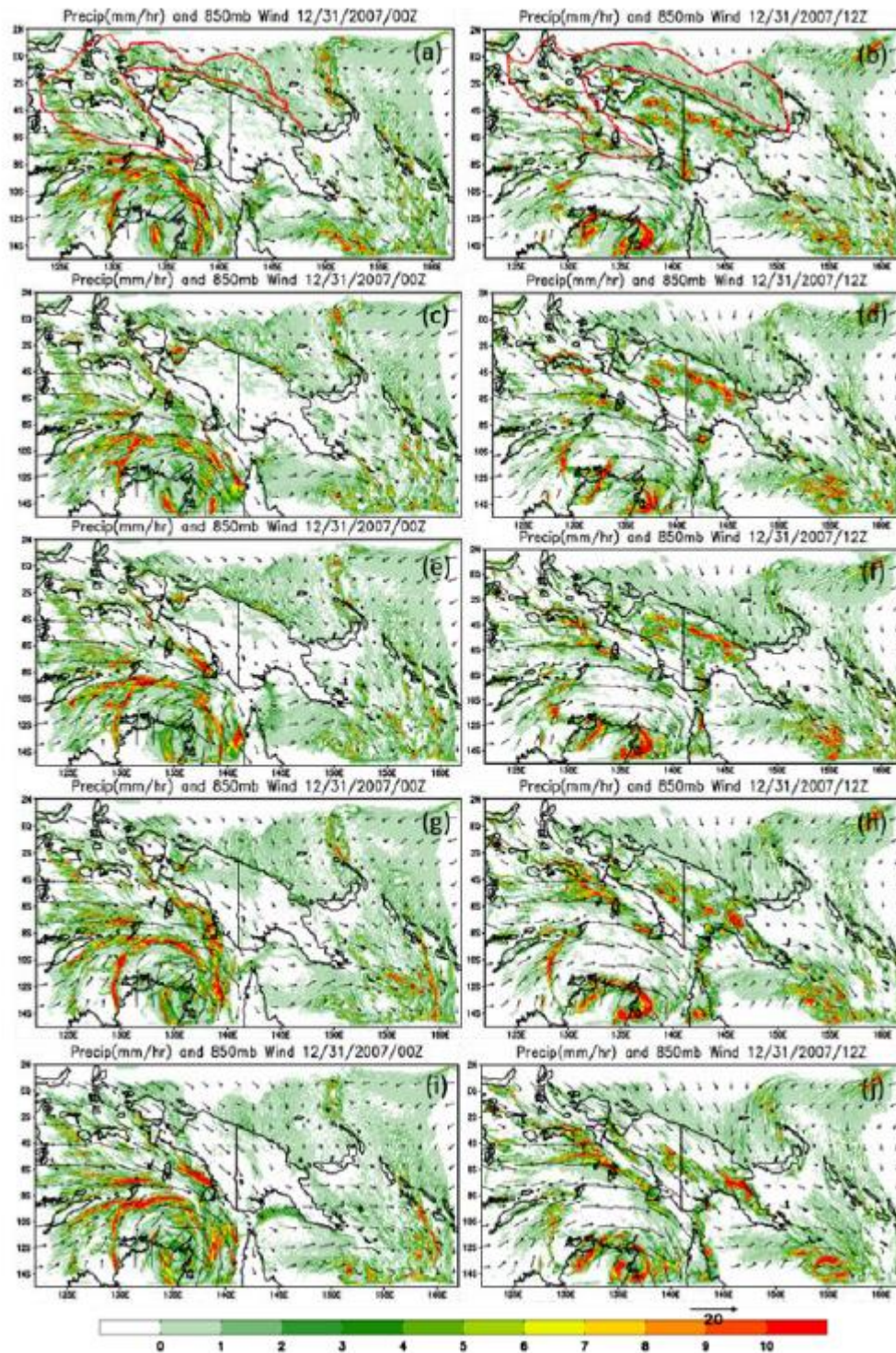

Figure 14. The 3-hour Rainfall and 850mb wind during the blocking stage of MJO07-08 for each of the varying height sensitivity test. CNTL (a,b), 75MT (c,d), 50MT (e,f), 25MT (g,h), NoMT (i,j)

In investigating whether there is w_{oro} associated with the MJO propagating over the NGH, we check to see if the high mountain or steepness of the orography of the NGH is enough to produce orographic rainfall. The slope is

estimated by using the mountain slope represented in the 5 km grid resolution of the simulation. The selected area's slope: the NW corner of the island of New Guinea, is ~ 0.060 (3.5km/58km), which is considered a steep mountain slope for the production of orographic rainfall. Meaning that w_{oro} is an ingredient for orographic rainfall. We can also verify this by looking at Fig. 14. As the steepness of the mountain changes, there is a change in the amount of rainfall produced.

Next, we want to see if w_{env} is an ingredient for orographic rainfall. The w_{env} refers to the release of conditional instability – large CAPE, potential instability, low-level convergence, and upper-level divergence present in the environment. Agyakwah and Lin (2020) found that CAPE played an essential role in producing heavy orographic rainfall. In the case of the MJO07-08, we see a large amount of CAPE, which would cause conditional instability during the blocking stage as the MJO propagates over the NHG (Fig. 15). This means that CAPE plays a significant role in the strong w_{env} and produces heavy orographic rainfall. Furthermore, the vapor mixing ratio in the area is about 20 g/kg, where the orographic terrain is blocking the MJO (Fig. 15). This amount is preferable for the production of heavy orographic rainfall, as shown in Agyakwah and Lin (2020).
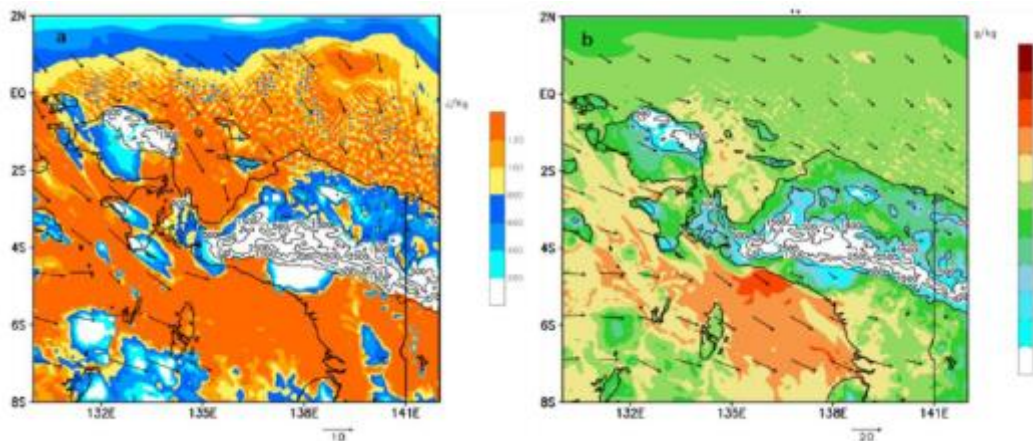

Figure 15. (a) CAPE from the surface to 850 hPa (b) water vapor mixing ratio (q_v)

With both the w_{oro} and w_{env} being ingredients, we want to see which ingredient plays a large role in the production of orographic rainfall. To do this, we compare the w_{oro} and w_{env} to the total upward motion associated with the MJO07-08 propagating over the NGH (Fig. 16). The result shows that most of the total upward motion associated with the MJO07-08 propagating over the NGH during the blocking stage is caused by the w_{env} and not the w_{oro}. Therefore, these results show that the w_{env} plays a large role in the production of orographic rainfall. However, this does not mean that the w_{oro} does not affect the production of orographic rainfall. These results show that the w_{env} has a much large effect on the production that the w_{oro}. We can also verify these results by looking at the vertical velocity (w) along the NW corner of the island of New Guinea and NGH.
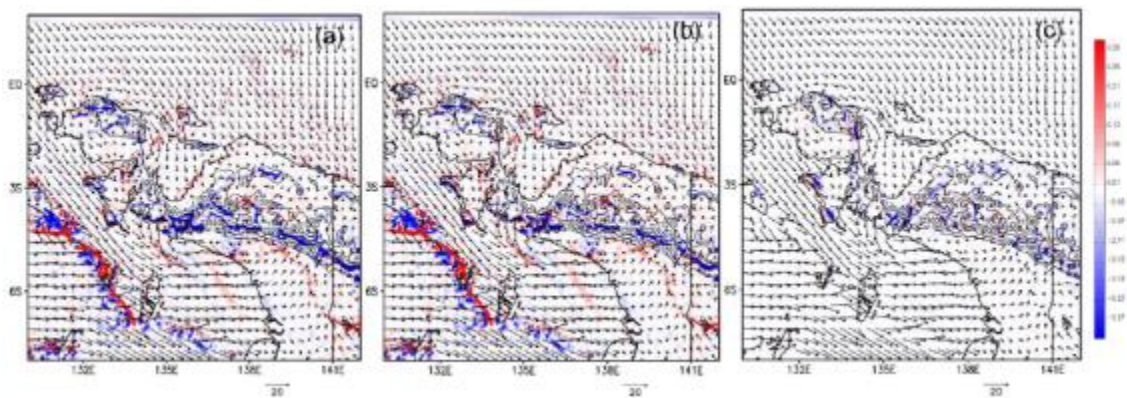

Figure 16. (a) The total upward motion for the NW corner during the blocking stage, (b) the environmental upward motion, and (c) the orographic upward motion

When looking at the w for each case (Fig. 17), we can see that during the blocking stage of the MJO07-08, there

is a strong w off the main island's coast, and strong downward motion is located on the island along the NGH in the CNTL case. As the mountain height is decreased, the strong upward motion moves more inland for each of the cases. We can also see that when the mountain height decreases, the strong downward motion mixes with the strong upward motion and reduces the amount of w present around the NGH. This reduction causes a reduction in the amount of orographic rainfall produced as the MJO propagates over the NGH as there is a reduction of w_{oro} and w_{env}.
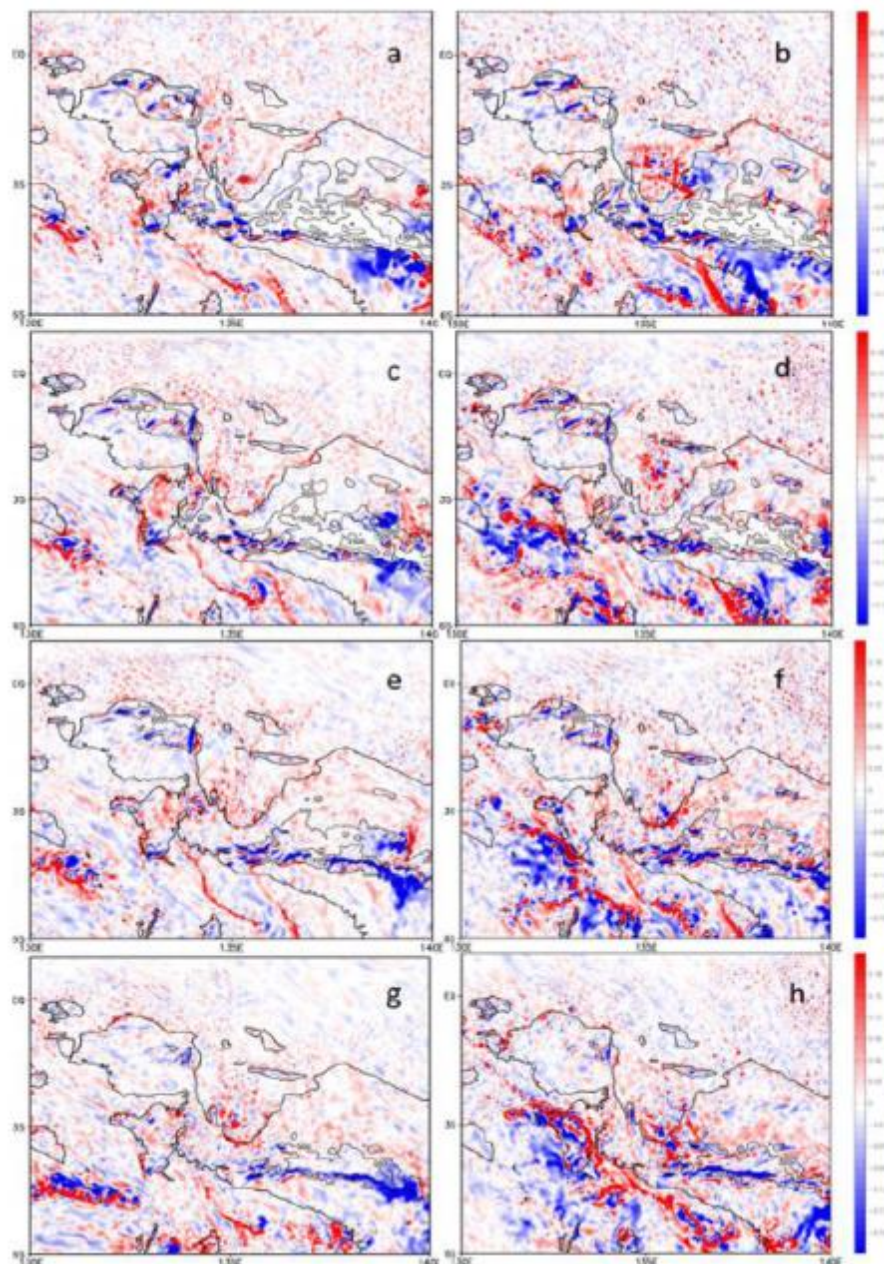
Figure 17. The vertical motion during the blocking stage for each varying height case. CNTL (a,b), 75MT(c,d), 50MT(e,f), 25MT (g,h)

This can be verified when looking at the convergence/divergence near the blocking area (Fig. 18). During the CNTL, there is strong convergence where we see the strong upward motion in Fig. 17. There is also strong divergence along the peninsula part of the main island. The strong divergence along the peninsula moves inward toward the main island as the mountain height decreases. We can also see that the strong convergence begins to spread along the island's coast as the mountain height decreases. Strong divergence reduces the orographic rainfall produced by the moist air lifted upward along the mountain. Based on the ingredients that were defined

by Lin (2007), we can confirm that the ingredients for the production of orographic rainfall associated with the MJO07-08 are (1) strong w_{oro} due to the steepness of the NGH, (2) conditional instability due to a large amount of CAPE, (3) very high water vapor mixing ratio, (4) strong w_{env}, (5) large convective system and, (6) a slow-moving MJO system.
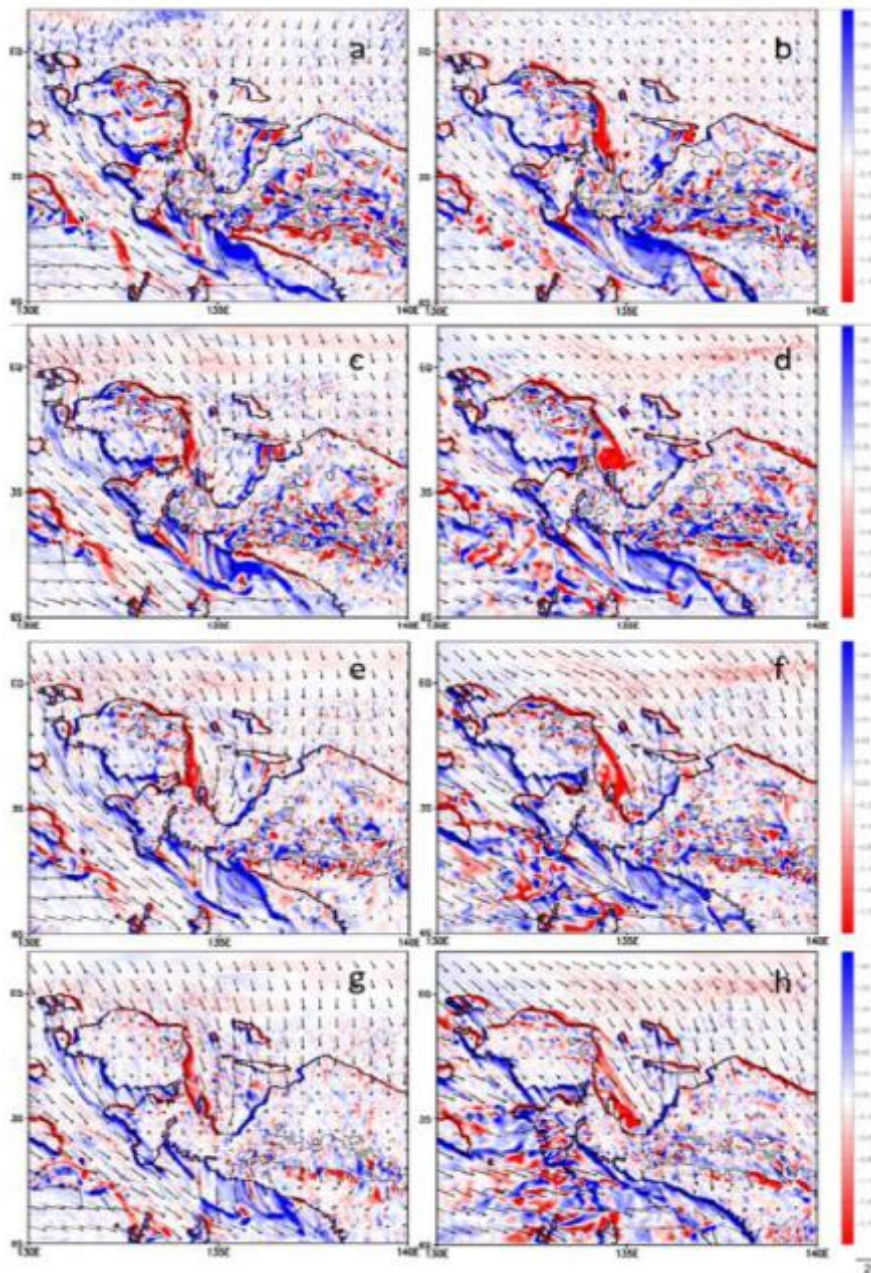

Figure 18. The convergence and divergence vorticity fields during the blocking stage for each varying height case

4. Concluding Remarks

In this study, we will use the Advanced Research Weather Research and Forecasting (WRF) model (Skamarock et al., 2019) to examine the orographic and thermal effects of the NGH on MJO propagation and rainfall over the island of New Guinea. When looking at the mechanical and diurnal thermal forces, the results from the WRF analysis show that both forces e affect propagation and rainfall during the blocking and splitting stages associated with the MJO07-08. However, the mechanical force has a large impact on the production of orographic rainfall compared to the diurnal thermal forces. We can conclude this when looking at NoMT and NoHT case results. With the NoMT case, we can see that the diurnal thermal forces are not strong enough to

completely block the MJO07-08 during the blocking stage. Likewise, when looking at the NoHT case, we can see that the mechanical forces are strong enough to block and split the MJO07-08 during the blocking and splitting stages. We also use the NMNH to show what happens when no forces interact with the MJO07-08 event. As a result, the MJO propagates over the island without any problems and does not produce any rainfall on the island itself. These are the expected results since no forces are present in the WRF model.

We also show that two flow regimes are associated with MJO07-08 during the blocking stage. The flow-around regime sees the convective system associated with the MJO splitting around the NGH due to the strong orographic blocking. We can observe this splitting when looking at the splitting stage. The flow-around regimes occur when the mountain height exceeds 50% of the original. There is also an increase in orographic rainfall as the mountain height increases. The flow-over regime occurs when the mountain is below 50% of the original mountain height. The convective system moves over the NGH with minimum to no blocking from the orographic terrain. When the mountain is at exactly 50%, the convective system occurs in flow-around and flow-over regimes. The flow regimes also show that orographic rainfall increases linearly until the mountain reaches 75% of the original height. We can see a plateau in the amount of rainfall produced once the mountain height begins to reach the original height. We see a decrease in the amount of rainfall produced.

Finally, we determine the orographic ingredients associated with the MJO07-08 event. Although the MJO is not a rotating convective like a hurricane, we can still determine the ingredients for the production of orographic rainfall. For the MJO07-08 event, we found that the ingredients responsible for the production of orographic rainfall are (1) strong w_{oro} due to the steepness of the NGH, (2) conditional instability due to a large amount of CAPE, (3) very high water vapor mixing ratio, (4) strong w_{env}, (5) large convective system and, (6) a slow-moving MJO system. We have also found that the w_{env} plays a much larger role than w_{oro} when looking at the role than w_{oro} when looking at the total upward motion associated with the MJO07-08 interacting with the NGH.

Acknowledgments

References

Agyakwah, W., & Lin, Y.-L. (2021). Generation and enhancement mechanisms for extreme orographic rainfall associated with Typhoon Morakot (2009) over the Central Mountain Range of Taiwan. *Atmospheric Research, 247*, 105160. https://doi.org/10.1016/j.atmosres.2020.105160

Buzzi, A., Tartaglione, N., & Malguzzi, P. (1998). Numerical Simulations of the 1994 Piedmont Flood: Role of Orography and Moist Processes. *Monthly Weather Review, 126*(9), 2369-2383. https://doi.org/10.1175/1520-0493(1998)126<2369:nsotpf>2.0.co;2

Chen, S.-H., & Lin, Y.-L. (2004). Orographic effects on a conditionally unstable flow over an idealized three-dimensional mesoscale mountain. *Meteorology and Atmospheric Physics, 88*(1-2), 1-21. https://doi.org/10.1007/s00703-003-0047-6

Chen, S.-H., & Lin, Y.-L. (2005). Effects of Moist Froude Number and CAPE on a Conditionally Unstable Flow over a Mesoscale Mountain Ridge. *Journal of the Atmospheric Sciences, 62*(2), 331-350. https://doi.org/10.1175/jas-3380.1

Chen, S.-H., Lin, Y.-L., & Zhao, Z. (2008). Effects of Unsaturated Moist Froude Number and Orographic Aspect Ratio on a Conditionally Unstable Flow over a Mesoscale Mountain. *Journal of the Meteorological Society of Japan. Ser. II, 86*(2), 353-367. https://doi.org/10.2151/jmsj.86.353

Chiao, S., & Lin, Y.-L. (2003). Numerical Modeling of an Orographically Enhanced Precipitation Event Associated with Tropical Storm Rachel over Taiwan. *Weather and Forecasting, 18*(2), 325-344. https://doi.org/10.1175/1520-0434(2003)018<0325:nmoaoe>2.0.co;2

Chu, C.-M., & Lin, Y.-L. (2000). Effects of Orography on the Generation and Propagation of Mesoscale Convective Systems in a Two-Dimensional Conditionally Unstable Flow. *Journal of the Atmospheric Sciences, 57*(23), 3817-3837. https://doi.org/10.1175/1520-0469(2001)057<3817:eoootg>2.0.co;2

Doswell, C. A., Brooks, H. E., & Maddox, R. A. (1996). Flash Flood Forecasting: An Ingredients-Based

Methodology. *Weather and Forecasting, 11*(4), 560-581. https://doi.org/10.1175/1520-0434(1996)011<0560:fffaib>2.0.co;2

Emanuel, K. A. (1994). *Atmospheric convection*. Oxford University Press. pp. 580.

Hsu, H.-H., & Lee, M.-Y. (2005). Topographic Effects on the Eastward Propagation and Initiation of the Madden-Julian Oscillation. *Journal of Climate, 18*(6), 795-809. https://doi.org/10.1175/jcli-3292.1

Huang, Y.-C., & Lin, Y.-L. (2013). A study on the structure and precipitation of Morakot (2009) induced by the Central Mountain Range of Taiwan. *Meteorology and Atmospheric Physics, 123*(3-4), 115-141. https://doi.org/10.1007/s00703-013-0290-4

Inness, P. M., & Slingo, J. M. (2006). The interaction of the Madden-Julian Oscillation with the Maritime Continent in a GCM. *Quarterly Journal of the Royal Meteorological Society, 132*(618), 1645-1667. https://doi.org/10.1256/qj.05.102

Jiang, L.-C. (2012). *The interaction between the MJO and topography: Using high-resolution data*. Master Thesis, Department of Atmospheric Sciences, National Taiwan University. pp. 82.

Kim, D., Kim, H., & Lee, M. (2017). Why does the MJO detour the Maritime Continent during austral summer? *Geophysical Research Letters, 44*(5), 2579-2587. https://doi.org/10.1002/2017gl072643

Ling, J., Zhang, C., Joyce, R., Xie, P., & Chen, G. (2019). Possible Role of the Diurnal Cycle in Land Convection in the Barrier Effect on the MJO by the Maritime Continent. *Geophysical Research Letters, 46*(5), 3001-3011. https://doi.org/10.1029/2019gl081962

Lin, Y.-L. (2010). *Mesoscale dynamics*. Cambridge University Press. pp. 630.

Lin, Y.-L., Agyakwah, W., Riley, J. G., Hsu, H.-H., & Jiang, L.-C. (2020). Orographic effects on the propagation and rainfall modification associated with the 2007-08 Madden-Julian oscillation (MJO) past the New Guinea Highlands. *Meteorology and Atmospheric Physics, 133*(2), 359-378. https://doi.org/10.1007/s00703-020-00753-2

Miglietta, M. M., & Rotunno, R. (2009). Numerical Simulations of Conditionally Unstable Flows over a Mountain Ridge. *Journal of the Atmospheric Sciences, 66*(7), 1865-1885. https://doi.org/10.1175/2009jas2902.1

Monier, E., Weare, B. C., & Gustafson, W. I. (2009). The Madden-Julian oscillation wind-convection coupling and the role of moisture processes in the MM5 model. *Climate Dynamics, 35*(2-3), 435-447. https://doi.org/10.1007/s00382-009-0626-4

Rostom, R., & Lin, Y.-L. (2021). Common Ingredients and Orographic Rain Index (ORI) for Heavy Precipitation Associated with Tropical Cyclones Passing Over the Appalachian Mountains. *Earth Science Research, 10*(1), 32. https://doi.org/10.5539/esr.v10n1p32

Skamarock, W. C., Klemp, J. B., Dudhia, J., Gill, D. O., Liu, Z., Berner, J., … Huang, X.-Y. (2019). *A description of the Advanced Research WRF Model Version4*. UCAR/NCAR. https://doi.org/10.5065/1DFH-6P97

Smolarkiewicz, P. K., & Rotunno, R. (1989). Low Froude Number Flow Past Three-Dimensional Obstacles. Part I: Baroclinically Generated Lee Vortices. *Journal of the Atmospheric Sciences, 46*(8), 1154-1164. https://doi.org/10.1175/1520-0469(1989)046<1154:lfnfpt>2.0.co;2

Tseng, W.-L., Hsu, H.-H., Keenlyside, N., June Chang, C.-W., Tsuang, B.-J., Tu, C.-Y., & Jiang, L.-C. (2017). Effects of Surface Orography and Land-Sea Contrast on the Madden-Julian Oscillation in the Maritime Continent: A Numerical Study Using ECHAM5-SIT. *Journal of Climate*, *30*(23), 9725-9741. https://doi.org/10.1175/jcli-d-17-0051.1

Witcraft, N. C., Lin, Y.-L., & Kuo, Y.-H. (2005). Dynamics of Orographic Rain Associated with the Passage of a Tropical Cyclone over a Mesoscale Mountain. *Terrestrial, Atmospheric and Oceanic Sciences, 16*(5), 1133. https://doi.org/10.3319/tao.2005.16.5.1133(a)

Wu, C.-H., & Hsu, H.-H. (2009). Topographic Influence on the MJO in the Maritime Continent. *Journal of Climate, 22*(20), 5433-5448. https://doi.org/10.1175/2009jcli2825.1

Zhang, C., & Ling, J. (2017). Barrier Effect of the Indo-Pacific Maritime Continent on the MJO: Perspectives from Tracking MJO Precipitation. *Journal of Climate, 30*(9), 3439-3459. https://doi.org/10.1175/jcli-d-16-0614.1

Copyrights